Electronic Supplementary Material (ESI) for Journal of Materials Chemistry A
This journal is © The Royal Society of Chemistry 2013

Supplementary Information

Design principles for microporous organic solids from predictive computational screening

Lauren J. Abbott, Neil B. McKeown, and Coray M. Colina

Contents

1 Simulation Models **S3**
1.1 Numbered chemical structures . . . S3
Figure S1. Biphenyl-core OMIMs . . . S3
Figure S2. Triptycene-core OMIMs . . . S4
Figure S3. Spirobisfluorene-core OMIMs . . . S5
Figure S4. Propellane-core OMIMs . . . S6
1.2 Atom types and partial charges . . . S7
Table S1. OMIM-[2+5] . . . S7
Table S2. OMIM-[2+6] . . . S7
Table S3. OMIM-[2+7] . . . S8
Table S4. OMIM-[2+5–tBu] . . . S8
Table S5. OMIM-[1+8] . . . S9
Table S6. OMIM-[1+9] . . . S9
Table S7. OMIM-[1+10] . . . S10
Table S8. OMIM-[1+11] . . . S11
Table S9. OMIM-[1+8–tBu] . . . S11
Table S10. OMIM-[1+8–Ad] . . . S12
Table S11. OMIM-[1+9–tBu] . . . S12
Table S12. OMIM-[3+8] . . . S13
Table S13. OMIM-[3+9] . . . S13
Table S14. OMIM-[3+10] . . . S14
Table S15. OMIM-[3+11] . . . S14
Table S16. OMIM-[4+8] . . . S15
Table S17. OMIM-[4+9] . . . S15
Table S18. OMIM-[4+10] . . . S16
Table S19. OMIM-[4+11] . . . S16
Table S20. OMIM-[4+8–tBu] . . . S17
Table S21. OMIM-[4+8–Ad] . . . S17
Table S22. OMIM-[4+9–tBu] . . . S18

2 Simulation Methods **S19**
2.1 *Ab initio* calculations . . . S19
2.2 Molecular dynamics simulations . . . S19
2.3 Characterization . . . S19

3 Results and Discussion **S20**
3.1 Electrostatic charge sets . . . S20
Figure S5. Comparison of charges for the biphenyl-core OMIMs . . . S20
3.2 Helium pore volumes . . . S21
Figure S6. Geometric surface area versus helium pore volume for the array of OMIMs . . . S21
3.3 Apparent surface areas from BET theory . . . S22
Table S23. Geometric and BET surface areas for biphenyl-core OMIMs . . . S22
Figure S7. BET plots for biphenyl-core OMIMs . . . S22
3.4 Core flexibility measurements . . . S23
Figure S8. Illustrations of the coarse grain beads defined for the core structures . . . S23
Table S24. Definitions of coarse grain beads for core flexibility measurements . . . S23
Table S25. Definitions of core flexibility angles . . . S23
3.5 Surface areas . . . S24
Figure S9. Geometric surface areas of real and ideal rigid-body simulations . . . S24
Figure S10. Volumetric geometric surface areas of functionalized OMIMs . . . S24
3.6 Radial distribution functions . . . S25
Figure S11. RDFs of end-group centers . . . S25
Figure S12. RDFs of molecular centers . . . S26
3.7 Structure factors . . . S27
Figure S13. Structure factors grouped by end group geometries . . . S27

References **S28**

1 Simulation Models

1.1 Numbered chemical structures

In the following figures, the chemical structures of the core and end group units are given with atom numbers assigned corresponding to Tables S1–S22. The orientation of the end groups relative to the core is signified by (a) and (b).

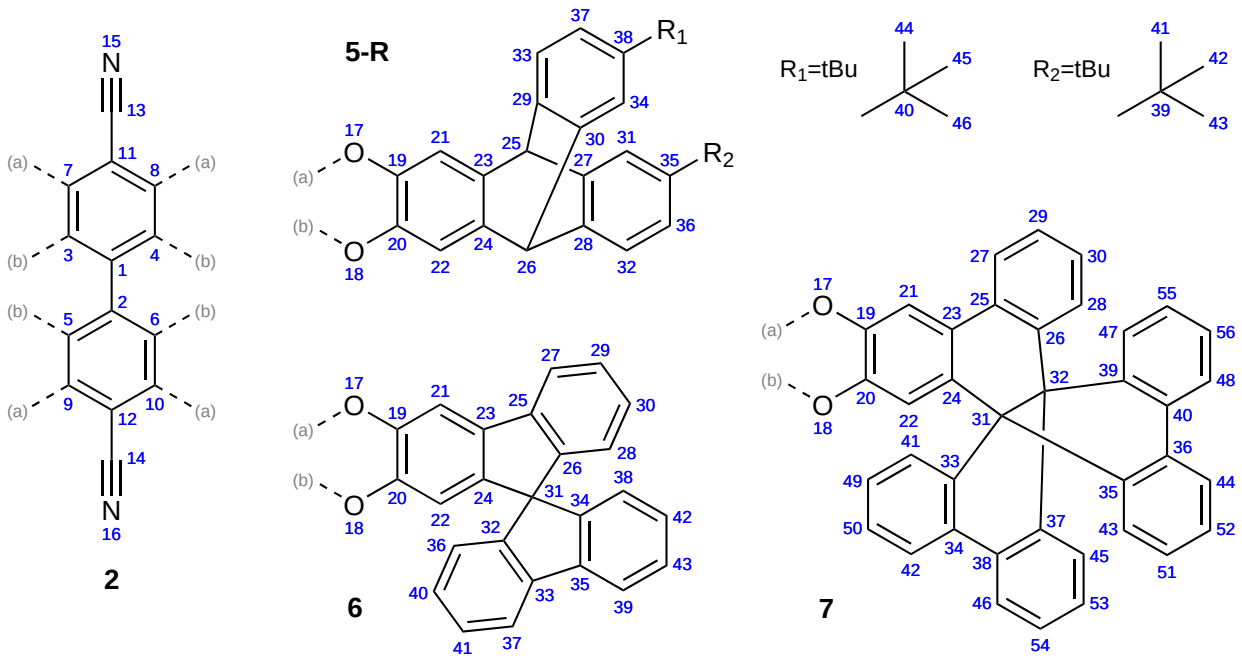

Figure S1. Biphenyl-core OMIMs.

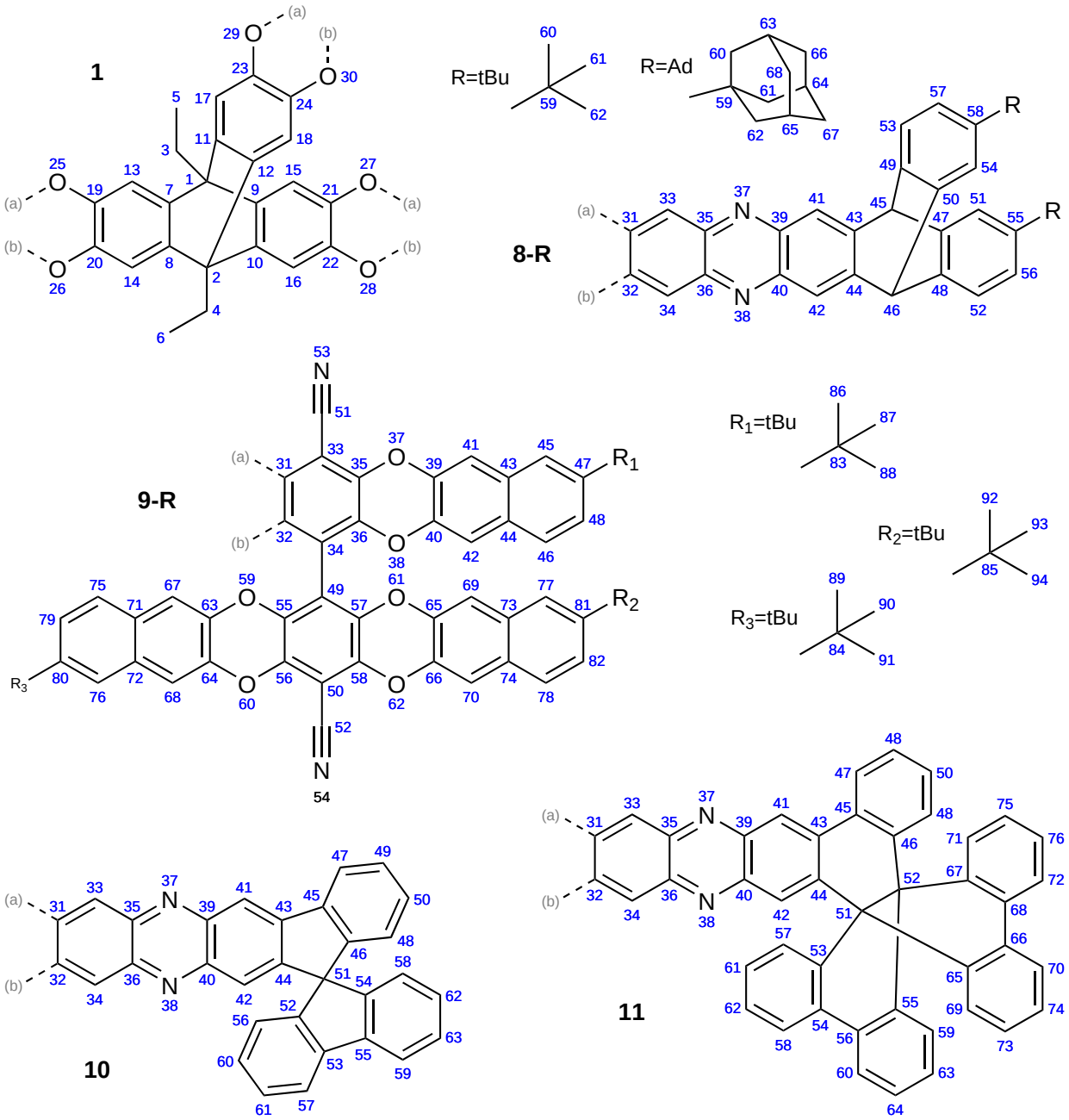

Figure S2. Triptycene-core OMIMs.

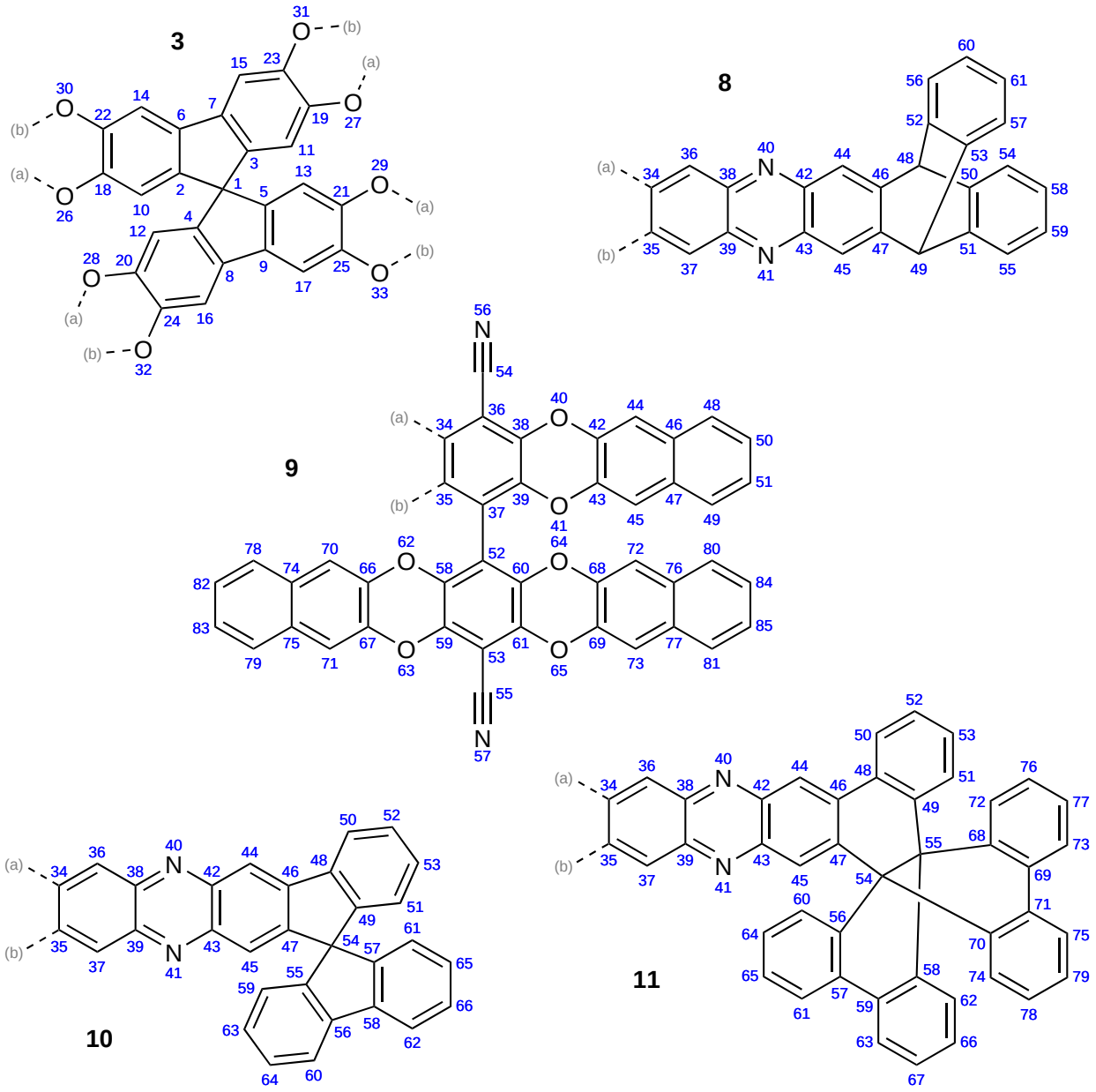

Figure S3. Spirobisfluorene-core OMIMs.

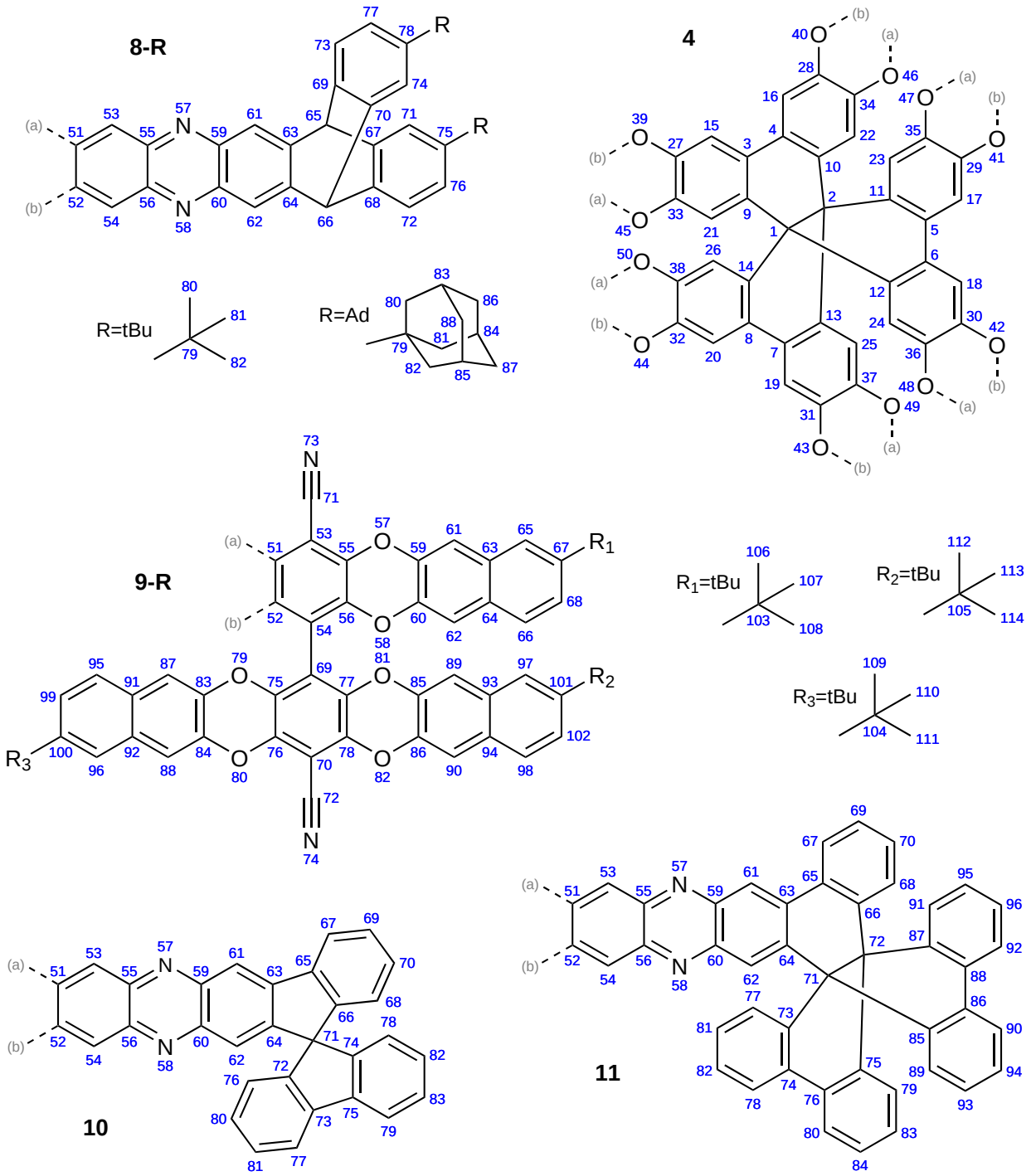

Figure S4. Propellane-core OMIMs.

1.2 Atom types and partial charges

In the following tables, the atom types and partial charges are given for all OMIMs. The atom numbers correspond to those labeled in Figures S1–S4, with hydrogen atoms identified by the starred number of their associated carbon atom. Atom types are from the polymer consistent force field (PCFF)[1] and partial charges were calculated as described in the methods section.

Table S1. OMIM-[2+5]

Number	Type	Charge (e)	Number	Type	Charge (e)	Number	Type	Charge (e)
1, 2	cp	+0.064843	21	cp	−0.280282	27, 29	cp	+0.003196
3–6	cp	+0.089862	21*	hc	+0.175883	28, 30	cp	+0.004811
7–10	cp	+0.109120	22	cp	−0.268300	31, 33	cp	−0.147784
11, 12	cp	−0.090177	22*	hc	+0.165751	31, 33*	hc	+0.128196
13, 14	ct	+0.332386	23	cp	+0.016358	32, 34	cp	−0.148705
15, 16	nt	−0.445222	24	cp	+0.010670	32, 34*	hc	+0.126654
17	oc	−0.200661	25	c1	+0.022919	35, 37	cp	−0.165366
18	oc	−0.204079	25*	hc	+0.104379	35, 37*	hc	+0.149256
19	cp	+0.192689	26	c1	+0.023050	36, 38	cp	−0.167756
20	cp	+0.146025	26*	hc	+0.102141	36, 38*	hc	+0.149278

Table S2. OMIM-[2+6]

Number	Type	Charge (e)	Number	Type	Charge (e)	Number	Type	Charge (e)
1, 2	cp	+0.039203	22*	hc	+0.183800	31	c	+0.013532
3–6	cp	+0.120005	23	cp	−0.003611	32, 34	cp	+0.051577
7–10	cp	+0.137259	24	cp	+0.002990	33, 35	cp	+0.038841
11, 12	cp	−0.123327	25	cp	+0.104010	36, 38	cp	−0.155295
13, 14	ct	+0.325337	26	cp	+0.022447	36, 38*	hc	+0.145430
15, 16	nt	−0.436685	27	cp	−0.191058	37, 39	cp	−0.192579
17	oc	−0.229903	27*	hc	+0.156891	37, 39*	hc	+0.148967
18	oc	−0.218378	28	cp	−0.179761	40, 42	cp	−0.168541
19	cp	+0.244699	28*	hc	+0.149203	40, 42*	hc	+0.148721
20	cp	+0.138702	29	cp	−0.168050	41, 43	cp	−0.147210
21	cp	−0.308947	29*	hc	+0.147520	41, 43*	hc	+0.146113
21*	hc	+0.191551	30	cp	−0.132051			
22	cp	−0.255999	30*	hc	+0.140837			

Table S3. OMIM-[2+7]

Number	Type	Charge (e)	Number	Type	Charge (e)	Number	Type	Charge (e)
1, 2	cp	+0.046024	25	cp	+0.043994	41, 43	cp	−0.081746
3–6	cp	+0.114378	26	cp	+0.043952	41, 43*	hc	+0.106230
7–10	cp	+0.131252	27	cp	−0.154619	42, 44	cp	−0.147861
11, 12	cp	−0.095012	27*	hc	+0.145618	42, 44*	hc	+0.133520
13, 14	ct	+0.309010	28	cp	−0.120334	45, 47	cp	−0.099367
15, 16	nt	−0.432788	28*	hc	+0.111520	45, 47*	hc	+0.113703
17	oc	−0.220638	29	cp	−0.173184	46, 48	cp	−0.156238
18	oc	−0.217529	29*	hc	+0.149590	46, 48*	hc	+0.136874
19	cp	+0.206679	30	cp	−0.149091	49, 51	cp	−0.184451
20	cp	+0.119948	30*	hc	+0.142543	49, 51*	hc	+0.149327
21	cp	−0.259903	31	c	+0.010530	50, 52	cp	−0.158685
21*	hc	+0.176314	32	c	+0.004293	50, 52*	hc	+0.146427
22	cp	−0.173647	33, 35	cp	+0.029377	53, 55	cp	−0.177745
22*	hc	+0.134930	34, 36	cp	+0.010913	53, 55*	hc	+0.146998
23	cp	−0.021335	37, 39	cp	+0.040410	54, 56	cp	−0.155559
24	cp	+0.016148	38, 40	cp	+0.015147	54, 56*	hc	+0.145213

Table S4. OMIM-[2+5–tBu]

Number	Type	Charge (e)	Number	Type	Charge (e)	Number	Type	Charge (e)
1, 2	cp	+0.072675	24	cp	+0.004473	34	cp	−0.188992
3–6	cp	+0.082022	25	c1	+0.045871	34*	hc	+0.122483
7–10	cp	+0.109015	25*	hc	+0.102634	35	cp	−0.048209
11, 12	cp	−0.088201	26	c1	+0.044375	36	cp	−0.195895
13, 14	ct	+0.331210	26*	hc	+0.101476	36*	hc	+0.148871
15, 16	nt	−0.445446	27	cp	−0.006091	37	cp	−0.200123
17	oc	−0.200575	28	cp	−0.005430	37*	hc	+0.151480
18	oc	−0.200936	29	cp	−0.006501	38	cp	−0.045688
19	cp	+0.194477	30	cp	−0.005885	39	c	+0.406803
20	cp	+0.142887	31	cp	−0.185839	40	c	+0.415290
21	cp	−0.276929	31*	hc	+0.125062	41–43	c3	−0.262943
21*	hc	+0.172928	32	cp	−0.174904	41–43*	hc	+0.056683
22	cp	−0.264465	32*	hc	+0.133706	44–46	c3	−0.260656
22*	hc	+0.162439	33	cp	−0.173319	44–46*	hc	+0.055085
23	cp	+0.008004	33*	hc	+0.135251			

Table S5. OMIM-[1+8]

Number	Type	Charge (e)	Number	Type	Charge (e)	Number	Type	Charge (e)
1, 2	c	−0.002285	25–30	oc	−0.292619	43, 44	cp	−0.013259
3, 4	c2	−0.049068	31, 32	cp	+0.239284	45, 46	c1	+0.003393
3, 4*	hc	+0.031445	33, 34	cp	−0.357011	45, 46*	hc	+0.111892
5, 6	c3	−0.076259	33, 34*	hc	+0.192396	47–50	cp	+0.012127
5, 6*	hc	+0.021574	35, 36	cp	+0.290740	51–54	cp	−0.145760
7–12	cp	+0.102533	37, 38	np	−0.478935	51–54*	hc	+0.127335
13–18	cp	−0.359826	39, 40	cp	+0.290681	55–58	cp	−0.166678
13–18*	hc	+0.206840	41, 42	cp	−0.241075	55–58*	hc	+0.149456
19–24	cp	+0.207653	41, 42*	hc	+0.144352			

Table S6. OMIM-[1+9]

Number	Type	Charge (e)	Number	Type	Charge (e)	Number	Type	Charge (e)
1, 2	c	−0.002285	38	oc	−0.208386	54	nt	−0.437088
3, 4	c2	−0.049068	39	cp	+0.229279	55, 57	cp	+0.145221
3, 4*	hc	+0.031445	40	cp	+0.121426	56, 58	cp	+0.192265
5, 6	c3	−0.076259	41	cp	−0.286859	59, 61	oc	−0.243729
5, 6*	hc	+0.021574	41*	hc	+0.182919	60, 62	oc	−0.237204
7, 9, 11	cp	+0.121596	42	cp	−0.251892	63, 65	cp	+0.164239
8, 10, 12	cp	+0.113701	42*	hc	+0.171024	64, 66	cp	+0.208314
13, 15, 17	cp	−0.384277	43	cp	+0.087000	67, 69	cp	−0.267570
13, 15, 17*	hc	+0.212929	44	cp	+0.075873	67, 69*	hc	+0.174176
14, 16, 18	cp	−0.374619	45	cp	−0.185594	68, 70	cp	−0.279513
14, 16, 18*	hc	+0.202351	45*	hc	+0.158191	68, 70*	hc	+0.184271
19, 21, 23	cp	+0.212256	46	cp	−0.193005	71, 73	cp	+0.076129
20, 22, 24	cp	+0.204401	46*	hc	+0.155442	72, 74	cp	+0.079044
25, 27, 29	oc	−0.226857	47	cp	−0.152472	75, 77	cp	−0.191748
26, 28, 30	oc	−0.262212	47*	hc	+0.150706	75, 77*	hc	+0.156117
31	cp	+0.174784	48	cp	−0.142704	76, 78	cp	−0.186348
32	cp	+0.148047	48*	hc	+0.149108	76, 78*	hc	+0.158166
33	cp	−0.202172	49	cp	+0.012695	79, 81	cp	−0.141144
34	cp	+0.027079	50	cp	−0.208401	79, 81*	hc	+0.148035
35	cp	+0.214166	51	ct	+0.342793	80, 82	cp	−0.145845
36	cp	+0.096617	52	ct	+0.349368	80, 82*	hc	+0.148837
37	oc	−0.243783	53	nt	−0.436856			

Table S7. OMIM-[1+10]

Number	Type	Charge (e)	Number	Type	Charge (e)	Number	Type	Charge (e)
1, 2	c	−0.002285	33*	hc	+0.196644	47*	hc	+0.164788
3, 4	c2	−0.049068	34	cp	−0.398183	48	cp	−0.173720
3, 4*	hc	+0.031445	34*	hc	+0.202741	48*	hc	+0.152926
5, 6	c3	−0.076259	35	cp	+0.302160	49	cp	−0.178177
5, 6*	hc	+0.021574	36	cp	+0.313980	49*	hc	+0.153162
7, 9, 11	cp	+0.104588	37	np	−0.488112	50	cp	−0.120250
8, 10, 12	cp	+0.112055	38	np	−0.482305	50*	hc	+0.143374
13, 15, 17	cp	−0.382403	39	cp	+0.278797	51	c	+0.028412
13, 15, 17*	hc	+0.210408	40	cp	+0.265987	52, 54	cp	+0.055928
14, 16, 18	cp	−0.390677	41	cp	−0.231233	53, 55	cp	+0.044271
14, 16, 18*	hc	+0.212430	41*	hc	+0.146751	56, 58	cp	−0.177379
19, 21, 23	cp	+0.228399	42	cp	−0.210081	56, 58*	hc	+0.163666
20, 22, 24	cp	+0.245661	42*	hc	+0.162666	57, 59	cp	−0.199951
25, 27, 29	oc	−0.307354	43	cp	+0.000642	57, 59*	hc	+0.150752
26, 28, 30	oc	−0.316250	44	cp	−0.027791	60, 62	cp	−0.164204
31	cp	+0.248068	45	cp	+0.069399	60, 62*	hc	+0.147411
32	cp	+0.275970	46	cp	−0.002855	61, 63	cp	−0.143724
33	cp	−0.371272	47	cp	−0.184465	61, 63*	hc	+0.145790

Table S8. OMIM-[1+11]

Number	Type	Charge (e)	Number	Type	Charge (e)	Number	Type	Charge (e)
1, 2	c	−0.002285	42	cp	−0.128065	61*	hc	+0.150405
3, 4	c2	−0.049068	42*	hc	+0.095052	62	cp	−0.144446
3, 4*	hc	+0.031445	43	cp	−0.026104	62*	hc	+0.140881
5, 6	c3	−0.076259	44	cp	−0.041029	63	cp	−0.175062
5, 6*	hc	+0.021574	45	cp	+0.063210	63*	hc	+0.148400
7, 9, 11	cp	+0.131069	46	cp	+0.063566	64	cp	−0.152559
8, 10, 12	cp	+0.127524	47	cp	−0.164063	64*	hc	+0.144519
13, 15, 17	cp	−0.445758	47*	hc	+0.144836	65	cp	+0.083449
13, 15, 17*	hc	+0.228540	48	cp	−0.119141	66	cp	+0.042215
14, 16, 18	cp	−0.425856	48*	hc	+0.123326	67	cp	+0.025292
14, 16, 18*	hc	+0.220948	49	cp	−0.153676	68	cp	+0.003223
19, 21, 23	cp	+0.250556	49*	hc	+0.144765	69	cp	−0.094513
20, 22, 24	cp	+0.233695	50	cp	−0.173266	69*	hc	+0.114151
25, 27, 29	oc	−0.292872	50*	hc	+0.147368	70	cp	−0.170827
26, 28, 30	oc	−0.275741	51	c	−0.005786	70*	hc	+0.134447
31	cp	+0.288505	52	c	+0.005187	71	cp	−0.111491
32	cp	+0.218461	53	cp	+0.021095	71*	hc	+0.113962
33	cp	−0.469879	54	cp	+0.002907	72	cp	−0.163871
33*	hc	+0.219093	55	cp	+0.026497	72*	hc	+0.141435
34	cp	−0.399609	56	cp	+0.015130	73	cp	−0.192668
34*	hc	+0.202875	57	cp	−0.074932	73*	hc	+0.148423
35	cp	+0.369832	57*	hc	+0.102354	74	cp	−0.137905
36	cp	+0.303179	58	cp	−0.151608	74*	hc	+0.140782
37	np	−0.499447	58*	hc	+0.137887	75	cp	−0.166636
38	np	−0.462690	59	cp	−0.118668	75*	hc	+0.144409
39	cp	+0.305010	59*	hc	+0.122423	76	cp	−0.143181
40	cp	+0.251775	60	cp	−0.155301	76*	hc	+0.140844
41	cp	−0.240523	60*	hc	+0.134956			
41*	hc	+0.146382	61	cp	−0.187667			

Table S9. OMIM-[1+8–tBu]

Number	Type	Charge (e)	Number	Type	Charge (e)	Number	Type	Charge (e)
1, 2	c	−0.002286	33, 34	cp	−0.426502	48, 49	cp	+0.000631
3, 4	c2	−0.049068	33, 34*	hc	+0.210427	51, 54	cp	−0.152073
3, 4*	hc	+0.031445	35, 36	cp	+0.324069	51, 54*	hc	+0.113803
5, 6	c3	−0.076259	37, 38	np	−0.485281	52, 53	cp	−0.142313
5, 6*	hc	+0.021574	39, 40	cp	+0.302815	52, 53*	hc	+0.129811
7–12	cp	+0.114092	41, 42	cp	−0.282669	55, 58	cp	−0.033797
13–18	cp	−0.395945	41, 42*	hc	+0.153525	56, 57	cp	−0.239065
13–18*	hc	+0.215339	43, 44	cp	+0.016946	56, 57*	hc	+0.163367
19–24	cp	+0.222404	45, 46	c1	−0.005673	59	c	+0.375216
25–30	oc	−0.286710	45, 46*	c1*	+0.115770	60–62	c3	−0.242776
31, 32	cp	+0.256379	47, 50	cp	−0.009143	60–62*	hc	+0.052545

Table S10. OMIM-[1+8–Ad]

Number	Type	Charge (e)	Number	Type	Charge (e)	Number	Type	Charge (e)
1, 2	c	−0.002288	35, 36	cp	+0.319315	52, 53*	hc	+0.135322
3, 4	c2	−0.049068	37, 38	np	−0.490793	55, 58	cp	−0.037010
3, 4*	hc	+0.031445	39, 40	cp	+0.305565	56, 57	cp	−0.198449
5, 6	c3	−0.076259	41, 42	cp	−0.274070	56, 57*	hc	+0.146552
5, 6*	hc	+0.021574	41, 42*	hc	+0.151280	59	c	+0.187335
7–12	cp	+0.116495	43, 44	cp	+0.010010	60–62	c2	−0.045505
13–18	cp	−0.399572	45, 46	c1	−0.007578	60–62*	hc	+0.009200
13–18*	hc	+0.215236	45, 46*	hc	+0.115017	63–65	c1	+0.050045
19–24	cp	+0.226008	47, 50	cp	+0.017267	63–65*	hc	−0.011863
25–30	oc	−0.288133	48, 49	cp	+0.005413	66–68	c2	−0.056989
31, 32	cp	+0.247348	51, 54	cp	−0.202598	66–68*	hc	+0.013322
33, 34	cp	−0.409398	51, 54*	hc	+0.130097			
33, 34*	hc	+0.207199	52, 53	cp	−0.170053			

Table S11. OMIM-[1+9–tBu]

Number	Type	Charge (e)	Number	Type	Charge (e)	Number	Type	Charge (e)
1, 2	c	−0.002285	45	cp	−0.149860	70	cp	−0.290432
3, 4	c2	−0.049068	45*	hc	+0.135293	70*	hc	+0.185673
3, 4*	hc	+0.031445	46	cp	−0.141350	71	cp	+0.056481
5, 6	c3	−0.076259	46*	hc	+0.146122	72	cp	+0.030116
5, 6*	hc	+0.021574	47	cp	−0.024918	73	cp	+0.033495
7, 9, 11	cp	+0.119993	48	cp	−0.251910	74	cp	+0.061144
8, 10, 12	cp	+0.102577	48*	hc	+0.168948	75	cp	−0.140062
13, 15, 17	cp	−0.365681	49	cp	+0.022528	75*	hc	+0.147040
13, 15, 17*	hc	+0.208214	50	cp	−0.170150	76	cp	−0.145065
14, 16, 18	cp	−0.346329	51	ct	+0.334525	76*	hc	+0.133005
14, 16, 18*	hc	+0.195810	52	ct	+0.337241	77	cp	−0.149007
19, 21, 23	cp	+0.202657	53	nt	−0.436297	77*	hc	+0.127098
20, 22, 24	cp	+0.182890	54	nt	−0.435560	78	cp	−0.140567
25, 27, 29	oc	−0.223800	55	cp	+0.129830	78*	hc	+0.149735
26, 28, 30	oc	−0.260159	56	cp	+0.186296	79	cp	−0.249778
31	cp	+0.149335	57	cp	+0.134718	79*	hc	+0.168378
32	cp	+0.167195	58	cp	+0.163454	80	cp	−0.023552
33	cp	−0.159376	59	oc	−0.257672	81	cp	−0.029961
34	cp	+0.012347	60	oc	−0.249630	82	cp	−0.248865
35	cp	+0.170366	61	oc	−0.228964	82*	hc	+0.170433
36	cp	+0.114010	62	oc	−0.243707	83	c	+0.370916
37	oc	−0.253191	63	cp	+0.184646	84	c	+0.356692
38	oc	−0.203869	64	cp	+0.241053	85	c	+0.375531
39	cp	+0.283270	65	cp	+0.169708	86–88	c3	−0.248798
40	cp	+0.117092	66	cp	+0.236309	86–88*	hc	+0.055829
41	cp	−0.318537	67	cp	−0.269588	89–91	c3	−0.240814
41*	hc	+0.189695	67*	hc	+0.170266	89–91*	hc	+0.054552
42	cp	−0.259784	68	cp	−0.303826	92–94	c3	−0.242859
42*	hc	+0.168823	68*	hc	+0.189431	92–94*	hc	+0.053741
43	cp	+0.035340	69	cp	−0.285126			
44	cp	+0.063576	68*	hc	+0.177593			

Table S12. OMIM-[3+8]

Number	Type	Charge (e)	Number	Type	Charge (e)	Number	Type	Charge (e)
1	c	+0.188868	37	cp	−0.395889	48*	hc	+0.117564
2–5	cp	+0.050372	37*	hc	+0.204389	49	c1	−0.030641
6–9	cp	+0.061419	38	cp	+0.308979	49*	hc	+0.118614
10–13	cp	−0.464016	39	cp	+0.311776	50, 52	cp	+0.027239
10–13*	hc	+0.241889	40	np	−0.477222	51, 53	cp	+0.032001
14–17	cp	−0.334057	41	np	−0.479138	54, 56	cp	−0.161994
14–17*	hc	+0.205851	42	cp	+0.299581	54, 56*	hc	+0.129155
18–21	cp	+0.351910	43	cp	+0.303008	55, 57	cp	−0.161078
22–25	cp	+0.172975	44	cp	−0.268328	55, 57*	hc	+0.129523
26–29	oc	−0.327836	44*	hc	+0.148414	58, 60	cp	−0.156043
30–33	oc	−0.269731	45	cp	−0.275751	58, 60*	hc	+0.145555
34	cp	+0.275302	45*	hc	+0.153726	59, 61	cp	−0.159455
35	cp	+0.221593	46	cp	+0.012742	59, 61*	hc	+0.145766
36	cp	−0.421509	47	cp	+0.006259			
36*	hc	+0.213641	48	c1	−0.024441			

Table S13. OMIM-[3+9]

Number	Type	Charge (e)	Number	Type	Charge (e)	Number	Type	Charge (e)
1	c	+0.201672	44	cp	−0.486050	59, 61	cp	+0.192265
2–5	cp	+0.061598	44*	hc	+0.232380	62, 64	oc	−0.243729
6–9	cp	+0.066739	45	cp	−0.385335	63, 65	oc	−0.237204
10–13	cp	−0.470797	45*	hc	+0.203396	66, 68	cp	+0.164239
10–13*	hc	+0.243043	46	cp	+0.160189	67, 69	cp	+0.208314
14–17	cp	−0.327811	47	cp	+0.150911	70, 72	cp	−0.267570
14–17*	hc	+0.199438	48	cp	−0.158795	70, 72*	hc	+0.174176
18–21	cp	+0.369291	48*	hc	+0.146458	71, 73	cp	−0.279513
22–25	cp	+0.119088	49	cp	−0.224245	71, 73*	hc	+0.184271
26–29	oc	−0.239030	49*	hc	+0.157112	74, 76	cp	+0.076129
30–33	oc	−0.189198	50	cp	−0.181570	75, 77	cp	+0.079044
34	cp	+0.094656	50*	hc	+0.151022	78, 80	cp	−0.191748
35	cp	+0.084756	51	cp	−0.116356	78, 80*	hc	+0.156117
36	cp	−0.153609	51*	hc	+0.141214	79, 81	cp	−0.186348
37	cp	+0.080805	52	cp	+0.012695	79, 81*	hc	+0.158166
38	cp	+0.173633	53	cp	−0.208401	82, 84	cp	−0.141144
39	cp	+0.043087	54	ct	+0.394427	82, 84*	hc	+0.148035
40	oc	−0.261464	55	ct	+0.349368	83, 85	cp	−0.145845
41	oc	−0.199336	56	nt	−0.463687	83, 85*	hc	+0.148837
42	cp	+0.358262	57	nt	−0.437088			
43	cp	+0.175360	58, 60	cp	+0.145221			

Table S14. OMIM-[3+10]

Number	Type	Charge (e)	Number	Type	Charge (e)	Number	Type	Charge (e)
1	c	+0.190016	38	cp	+0.315517	51*	hc	+0.146211
2–5	cp	+0.050654	39	cp	+0.326637	52	cp	−0.167471
6–9	cp	+0.061503	40	np	−0.489447	52*	hc	+0.146920
10–13	cp	−0.465192	41	np	−0.482542	53	cp	−0.123978
10–13*	hc	+0.242284	42	cp	+0.316354	53*	hc	+0.139496
14–17	cp	−0.333761	43	cp	+0.274561	54	c	+0.022370
14–17*	hc	+0.206176	44	cp	−0.264786	55, 57	cp	+0.045224
18–21	cp	+0.353650	44*	hc	+0.153307	56, 58	cp	+0.047239
22–25	cp	+0.171996	45	cp	−0.215489	59, 61	cp	−0.175136
26–29	oc	−0.327928	45*	hc	+0.162383	59, 61*	hc	+0.153191
30–33	oc	−0.268875	46	cp	−0.031326	60, 62	cp	−0.198499
34	cp	+0.277120	47	cp	−0.021654	60, 62*	hc	+0.150946
35	cp	+0.223617	48	cp	+0.116176	63, 65	cp	−0.155687
36	cp	−0.425824	49	cp	+0.031216	63, 65*	hc	+0.146137
36*	hc	+0.215079	50	cp	−0.198922	64, 66	cp	−0.148143
37	cp	−0.403399	50*	hc	+0.163173	64, 66*	hc	+0.146468
37*	hc	+0.207351	51	cp	−0.174141			

Table S15. OMIM-[3+11]

Number	Type	Charge (e)	Number	Type	Charge (e)	Number	Type	Charge (e)
1	c	+0.178440	46	cp	−0.030826	64*	hc	+0.149916
2–5	cp	+0.055166	47	cp	−0.044609	65	cp	−0.173373
6–9	cp	+0.057970	48	cp	+0.044099	65*	hc	+0.149594
10–13	cp	−0.468289	49	cp	+0.047182	66	cp	−0.161949
10–13*	hc	+0.243045	50	cp	−0.146249	66*	hc	+0.144455
14–17	cp	−0.340798	50*	hc	+0.143299	67	cp	−0.161986
14–17*	hc	+0.207709	51	cp	−0.120230	67*	hc	+0.145491
18–21	cp	+0.351026	51*	hc	+0.123774	68	cp	+0.046329
22–25	cp	+0.198105	52	cp	−0.169537	69	cp	+0.013496
26–29	oc	−0.320173	52*	hc	+0.147422	70	cp	+0.050906
30–33	oc	−0.288258	53	cp	−0.157735	71	cp	+0.034338
34	cp	+0.254989	53*	hc	+0.144802	72	cp	−0.085169
35	cp	+0.229807	54	c	−0.009160	72*	hc	+0.109910
36	cp	−0.437980	55	c	−0.003101	73	cp	−0.166072
36*	hc	+0.216655	56	cp	+0.048543	73*	hc	+0.140054
37	cp	−0.370590	57	cp	+0.026197	74	cp	−0.081467
37*	hc	+0.202397	58	cp	+0.010291	74*	hc	+0.106120
38	cp	+0.373604	59	cp	+0.005079	75	cp	−0.149655
39	cp	+0.269528	60	cp	−0.056628	75*	hc	+0.132006
40	np	−0.502416	60*	hc	+0.091118	76	cp	−0.190025
41	np	−0.480083	61	cp	−0.145497	76*	hc	+0.149295
42	cp	+0.277221	61*	hc	+0.133857	77	cp	−0.146645
43	cp	+0.308632	62	cp	−0.110704	77*	hc	+0.145068
44	cp	−0.215979	62*	hc	+0.116046	78	cp	−0.187726
44*	hc	+0.142642	63	cp	−0.143651	78*	hc	+0.149737
45	cp	−0.158248	63*	hc	+0.131523	79	cp	−0.161533
45*	hc	+0.111252	64	cp	−0.185954	79*	hc	+0.147990

Table S16. OMIM-[4+8]

Number	Type	Charge (e)	Number	Type	Charge (e)	Number	Type	Charge (e)
1, 2	c	+0.024414	54	cp	−0.386984	65*	hc	+0.109547
3–8	cp	+0.043454	54*	hc	+0.200833	66	c1	−0.015453
9–14	cp	+0.027565	55	cp	+0.320550	66*	hc	+0.111197
15–20	cp	−0.287019	56	cp	+0.292267	67, 69	cp	+0.023258
15–20*	hc	+0.180377	57	np	−0.468245	68, 70	cp	+0.022767
21–26	cp	−0.242266	58	np	−0.470373	71, 73	cp	−0.163724
21–26*	hc	+0.168487	59	cp	+0.271066	71, 73*	hc	+0.131868
27–32	cp	+0.210257	60	cp	+0.301216	72, 74	cp	−0.161648
33–38	cp	+0.202948	61	cp	−0.259470	72, 74*	hc	+0.132311
39–44	oc	−0.290364	61*	hc	+0.146904	75, 77	cp	−0.157984
45–50	oc	−0.295295	62	cp	−0.273899	75, 77*	hc	+0.146617
51	cp	+0.266322	62*	hc	+0.149623	76, 78	cp	−0.160250
52	cp	+0.243103	63	cp	+0.017430	76, 78*	hc	+0.147327
53	cp	−0.415796	64	cp	+0.018205			
53*	hc	+0.204953	65	c1	−0.010362			

Table S17. OMIM-[4+9]

Number	Type	Charge (e)	Number	Type	Charge (e)	Number	Type	Charge (e)
1, 2	c	+0.000000	61	cp	−0.286859	76, 78	cp	+0.192265
3–8	cp	+0.113701	61*	hc	+0.182919	79, 81	oc	−0.243729
9–14	cp	+0.121596	62	cp	−0.251892	80, 82	oc	−0.237204
15–20	cp	−0.374619	62*	hc	+0.171024	83, 85	cp	+0.164239
15–20*	hc	+0.202351	63	cp	+0.087000	84, 86	cp	+0.208314
21–26	cp	−0.384277	64	cp	+0.075873	87, 89	cp	−0.267570
21–26*	hc	+0.212929	65	cp	−0.185594	87, 89*	hc	+0.174176
27–32	cp	+0.204401	65*	hc	+0.158191	88, 90	cp	−0.279513
33–38	cp	+0.212256	66	cp	−0.193005	88, 90*	hc	+0.184271
39–44	oc	−0.262212	66*	hc	+0.155442	91, 93	cp	+0.076129
45–50	oc	−0.226857	67	cp	−0.152472	92, 94	cp	+0.079044
51	cp	+0.174784	67*	hc	+0.150706	95, 97	cp	−0.191748
52	cp	+0.148047	68	cp	−0.142704	95, 97*	hc	+0.156117
53	cp	−0.202172	68*	hc	+0.149108	96, 98	cp	−0.186348
54	cp	+0.027079	69	cp	+0.012695	96, 98*	hc	+0.158166
55	cp	+0.214166	70	cp	−0.208401	99, 101	cp	−0.141144
56	cp	+0.096617	71	ct	+0.342793	99, 101*	hc	+0.148035
57	oc	−0.243783	72	ct	+0.349368	100, 102	cp	−0.145845
58	oc	−0.208386	73	nt	−0.436856	100, 102*	hc	+0.148837
59	cp	+0.229279	74	nt	−0.437088			
60	cp	+0.121426	75, 77	cp	+0.145221			

Table S18. OMIM-[4+10]

Number	Type	Charge (e)	Number	Type	Charge (e)	Number	Type	Charge (e)
1, 2	c	+0.013674	55	cp	+0.299912	68*	hc	+0.148776
3–8	cp	+0.046306	56	cp	+0.313497	69	cp	−0.169387
9–14	cp	+0.029412	57	np	−0.473985	69*	hc	+0.147935
15–20	cp	−0.283102	58	np	−0.467145	70	cp	−0.112427
15–20*	hc	+0.179995	59	cp	+0.285969	70*	hc	+0.138554
21–26	cp	−0.250181	60	cp	+0.265749	71	c	+0.035397
21–26*	hc	+0.170546	61	cp	−0.257959	72, 74	cp	+0.041586
27–32	cp	+0.196745	61*	hc	+0.151252	73, 75	cp	+0.042463
33–38	cp	+0.220680	62	cp	−0.227006	76, 78	cp	−0.161251
39–44	oc	−0.287968	62*	hc	+0.159056	76, 78*	hc	+0.149467
45–50	oc	−0.300563	63	cp	−0.003220	77, 79	cp	−0.182062
51	cp	+0.253701	64	cp	−0.003702	77, 79*	hc	+0.145760
52	cp	+0.254647	65	cp	+0.096021	80, 82	cp	−0.159933
53	cp	−0.387887	66	cp	+0.017688	80, 82*	hc	+0.146666
53*	hc	+0.199363	67	cp	−0.203470	81, 83	cp	−0.158677
54	cp	−0.397457	67*	hc	+0.167208	81, 83*	hc	+0.148249
54*	hc	+0.202769	68	cp	−0.184813			

Table S19. OMIM-[4+11]

Number	Type	Charge (e)	Number	Type	Charge (e)	Number	Type	Charge (e)
1, 2	c	+0.000000	63	cp	−0.026104	81*	hc	+0.150405
3–8	cp	+0.127524	64	cp	−0.041029	82	cp	−0.144446
9–14	cp	+0.131069	65	cp	+0.063210	82*	hc	+0.140881
15–20	cp	−0.425856	66	cp	+0.063566	83	cp	−0.175062
15–20*	hc	+0.220948	67	cp	−0.164063	83*	hc	+0.148400
21–26	cp	−0.445758	67*	hc	+0.144836	84	cp	−0.152559
21–26*	hc	+0.228540	68	cp	−0.119141	84*	hc	+0.144519
27–32	cp	+0.233695	68*	hc	+0.123326	85	cp	+0.083449
33–38	cp	+0.250556	69	cp	−0.153676	86	cp	+0.042215
39–44	oc	−0.275741	69*	hc	+0.144765	87	cp	+0.025292
45–50	oc	−0.292872	70	cp	−0.173266	88	cp	+0.003223
51	cp	+0.288505	70*	hc	+0.147368	89	cp	−0.094513
52	cp	+0.218461	71	c	−0.005786	89*	hc	+0.114151
53	cp	−0.469879	72	c	+0.005187	90	cp	−0.170827
53*	hc	+0.219093	73	cp	+0.021095	90*	hc	+0.134447
54	cp	−0.399609	74	cp	+0.002907	91	cp	−0.111491
54*	hc	+0.202875	75	cp	+0.026497	91*	hc	+0.113962
55	cp	+0.369832	76	cp	+0.015130	92	cp	−0.163871
56	cp	+0.303179	77	cp	−0.074932	92*	hc	+0.141435
57	np	−0.499447	77*	hc	+0.102354	93	cp	−0.192668
58	np	−0.462690	78	cp	−0.151608	93*	hc	+0.148423
59	cp	+0.305010	78*	hc	+0.137887	94	cp	−0.137905
60	cp	+0.251775	79	cp	−0.118668	94*	hc	+0.140782
61	cp	−0.240523	79*	hc	+0.122423	95	cp	−0.166636
61*	hc	+0.146382	80	cp	−0.155301	95*	hc	+0.144409
62	cp	−0.128065	80*	hc	+0.134956	96	cp	−0.143181
62*	hc	+0.095052	81	cp	−0.187667	96*	hc	+0.140844

Table S20. OMIM-[4+8–tBu]

Number	Type	Charge (e)	Number	Type	Charge (e)	Number	Type	Charge (e)
1, 2	c	+0.000000	57, 58	np	−0.485281	71, 74*	hc	+0.113803
3–14	cp	+0.114092	59, 60	cp	+0.302815	72, 73	cp	−0.142313
15–26	cp	−0.395945	61, 62	cp	−0.282669	72, 73*	hc	+0.129811
15–26*	hc	+0.215339	61, 62*	hc	+0.153525	75, 78	cp	−0.033797
27–38	cp	+0.222404	63, 64	cp	+0.016946	76, 77	cp	−0.239065
39–50	oc	−0.286710	65, 66	c1	−0.005673	76, 77*	hc	+0.163367
51, 52	cp	+0.256379	65, 66*	hc	+0.115770	79	c	+0.375216
53, 54	cp	−0.426502	67, 70	cp	−0.009143	80–82	c3	−0.242776
53, 54*	hc	+0.210427	68, 69	cp	+0.000631	80–82*	hc	+0.052545
55, 56	cp	+0.324069	71, 74	cp	−0.152073			

Table S21. OMIM-[4+8–Ad]

Number	Type	Charge (e)	Number	Type	Charge (e)	Number	Type	Charge (e)
1, 2	c	+0.000000	59, 60	cp	+0.305565	72, 73*	hc	+0.135322
3–14	cp	+0.116495	61, 62	cp	−0.274070	75, 78	cp	−0.037010
15–26	cp	−0.399572	61, 62*	hc	+0.151280	76, 77	cp	−0.198449
15–26*	hc	+0.215236	63, 64	cp	+0.010010	76, 77*	hc	+0.146552
27–38	cp	+0.226008	65, 66	c1	−0.007578	79	c	+0.187335
39–50	oc	−0.288133	65, 66*	hc	+0.115017	80–82	c2	−0.045505
51, 52	cp	+0.247348	67, 70	cp	+0.017267	80–82*	hc	+0.009200
53, 54	cp	−0.409398	68, 69	cp	+0.005413	83–85	c1	+0.050045
53, 54*	hc	+0.207199	71, 74	cp	−0.202598	83–85*	hc	−0.011863
55, 56	cp	+0.319315	71, 74*	hc	+0.130097	86–88	c2	−0.056989
57, 58	np	−0.490793	72, 73	cp	−0.170053	86–88*	hc	+0.013322

Table S22. OMIM-[4+9–tBu]

Number	Type	Charge (e)	Number	Type	Charge (e)	Number	Type	Charge (e)
1, 2	c	+0.000000	66	cp	−0.141350	90	cp	−0.290432
3–8	cp	+0.119993	66*	hc	+0.146122	90*	hc	+0.185673
9–14	cp	+0.102577	67	cp	−0.024918	91	cp	+0.056481
15–20	cp	−0.365681	68	cp	−0.251910	92	cp	+0.030116
15–20*	hc	+0.208214	68*	hc	+0.168948	93	cp	+0.033495
21–26	cp	−0.346329	69	cp	+0.022528	94	cp	+0.061144
21–26*	hc	+0.195810	70	cp	−0.170150	95	cp	−0.140062
27–32	cp	+0.202657	71	ct	+0.334525	95*	hc	+0.147040
33–38	cp	+0.182890	72	ct	+0.337241	96	cp	−0.145065
39–44	oc	−0.223800	73	nt	−0.436297	96*	hc	+0.133005
45–50	oc	−0.260159	74	nt	−0.435560	97	cp	−0.149007
51	cp	+0.149335	75	cp	+0.129830	97*	hc	+0.127098
52	cp	+0.167195	76	cp	+0.186296	98	cp	−0.140567
53	cp	−0.159376	77	cp	+0.134718	98*	hc	+0.149735
54	cp	+0.012347	78	cp	+0.163454	99	cp	−0.249778
55	cp	+0.170366	79	oc	−0.257672	99*	hc	+0.168378
56	cp	+0.114010	80	oc	−0.249630	100	cp	−0.023552
57	oc	−0.253191	81	oc	−0.228964	101	cp	−0.029961
58	oc	−0.203869	82	oc	−0.243707	102	cp	−0.248865
59	cp	+0.283270	83	cp	+0.184646	102*	hc	+0.170433
60	cp	+0.117092	84	cp	+0.241053	103	c	+0.370916
61	cp	−0.318537	85	cp	+0.169708	104	c	+0.356692
61*	hc	+0.189695	86	cp	+0.236309	105	c	+0.375531
62	cp	−0.259784	87	cp	−0.269588	106–108	c3	−0.248798
62*	hc	+0.168823	87*	hc	+0.170266	106–108*	hc	+0.055829
63	cp	+0.035340	88	cp	−0.303826	109–111	c3	−0.240814
64	cp	+0.063576	88*	hc	+0.189431	109–111*	hc	+0.054552
65	cp	−0.149860	89	cp	−0.285126	112–114	c3	−0.242859
65*	hc	+0.135293	89*	hc	+0.177593	112–114*	hc	+0.053741

2 Simulation Methods

2.1 *Ab initio* calculations

Electrostatic potentials (ESP) were calculated in Gaussian 03[2] at the HF/6-31G* level of theory. A restrained electrostatic potential (RESP) charge fitting[3] was applied to determine the discrete partial charges from the ESP. Due to the large sizes of the molecules (152–698 atoms), the *ab initio* calculations were performed on fragments of the molecular structures, then pieced together for the whole molecule. For example, OMIM-[2+5] was broken in half at the single carbon–carbon bond of the biphenyl core, which was then capped with a methyl group. The ESP was then calculated for only half of the molecule, and the charges were assigned to both halves. Similar fragmenting was applied to the other molecules, making sure not to break the molecule across a conjugated structure. The discrete partial charges resulting from these calculations are given in Tables S1–S22, which correspond to the chemical structures in Figures S1–S4.

2.2 Molecular dynamics simulations

All molecular dynamics (MD) simulations were performed using LAMMPS[4,5] with a velocity-verlet integrator and a 1 fs timestep. The canonical (NVT) and isothermal-isobaric (NPT) ensembles were controlled with a Nosé-Hoover thermostat and barostat. Pairwise interactions were calculated with a cutoff of 15 Å and long-range electrostatic interactions were included using the particle-particle particle-mesh (PPPM) method.[6] The total length of the 21-step MD compression scheme performed was 1.56 nm, with the parameters $T_{\mathrm{max}} = 1000$ K, $P_{\mathrm{max}} = 5 \times 10^4$ bar, $T_{\mathrm{final}} = 300$ K, and $P_{\mathrm{final}} = 1$ bar.[7]

2.3 Characterization

Bulk densities, $\rho_{\mathrm{bulk}} = m/v_{\mathrm{tot}}$, were obtained using the total mass of the system, m, and total periodic simulation cell volume, $v_{\mathrm{tot}} = L^3$, where L is the length of the simulation cell.

Structure factors, $S(q)$, were calculated in ISAACS[8,9] from the Fourier transform of the radial distribution function, $g(r)$, which is related to the likelihood of finding atoms a distance r apart in the structure. Other structural characterization was provided by angle and distance measurements between atoms within the system. For the radial distribution functions calculated from end-group or molecular centers, half the box size was used as the cutoff. All of these calculations were averaged over 10 frames during a 500 ps NVT MD simulation of the equilibrated system.

Geometrical measures of the surface area, SA_{geom}, were obtained by a Monte Carlo integration technique using the Poreblazer code, where the molecular surface can be thought of being defined by a spherical probe "rolled" across the system atoms.[10] The accessible surface was taken from the center of a spherical probe the size of a nitrogen molecule ($d_{\mathrm{N2}} = 3.685$ Å), and the size of the system atoms were represented by their sigma values. A total of $N = 2000$ test points per atom was used for the calculations. In addition, helium pore volumes were obtained using the Widom insertion method in Poreblazer. A helium test probe ($\sigma = 2.58$ Å, $\epsilon = 10.22$ K) was considered at 298 K, with a total of $N = 5 \times 10^5$ insertions.

Gas adsorption isotherms were simulated using the MCCCS Towhee program.[11] Simulations were performed in the grand canonical ensemble (μVT) with the RANLUX pseudo-random number generator.[12,13] Nonbond parameters for nitrogen (N_2) were taken from TraPPE.[14] During the simulations, the OMIMs were held fixed, while gas molecules underwent insertion, deletion, translation, and rotation steps (1.5×10^7 steps for both equilibration and production).

Apparent surface areas were calculated from the simulated N_2 isotherms through application of BET theory,[15] SA_{BET}, as is done experimentally. The surface areas were derived from the linear region of the BET plot over the pressure range $0.01 \leq p/p_0 \leq 0.03$, which was obtained using the consistency criteria suggested by Rouquerol et al.[16] The monolayer area of nitrogen was assumed to be 16.2 Å^2.

3 Results and Discussion

3.1 Electrostatic charge sets

A comparison is provided here between the charge sets given by (i) a bond increments approach using PCFF and (ii) a fitting of the electrostatic potential via *ab initio* calculations. A direct comparison of the PCFF and *ab initio* charges for the atoms within the biphenyl-core OMIMs (Figure S1) is provided in Figure S5. In this plot, perfect agreement between the two sets of charges is represented by the diagonal line, such that the deviations of the PCFF charges from the *ab initio* charges are given by the separation of the points in the y-direction from that line. Points in the regions between the x-axis and diagonal line represent cases in which the PCFF charges are weaker than the *ab initio* charges. From this comparison, it is clear that, in general, PCFF provided weaker charges overall, as many of the points fall between the x-axis and diagonal line.

Specific atoms showing the greatest deviations are labeled in Figure S5, which mostly reside in the core structure. The largest discrepancies were observed for the polar nitrile groups, which are notably 3–9 times stronger in the *ab initio* calculations. In addition to the nitrile groups, large variations existed along the conjugated core structure. Given that PCFF charges only take into account the immediately bonded atoms, it is not surprising that this charge set is not able the capture the delocalization present along the aromatic ladder structure, which is more appropriately represented by the *ab initio* calculations. One other site of significant deviation was the central carbon atom of the *tert*-butyl groups of OMIM-[2+5–tBu]. While this carbon atom has a large positive charge, the net charge of the entire *tert*-butyl group is only weakly positive. Thus, it is believed that the *tert*-butyl groups do not provide strong electrostatic interactions in a packed state.

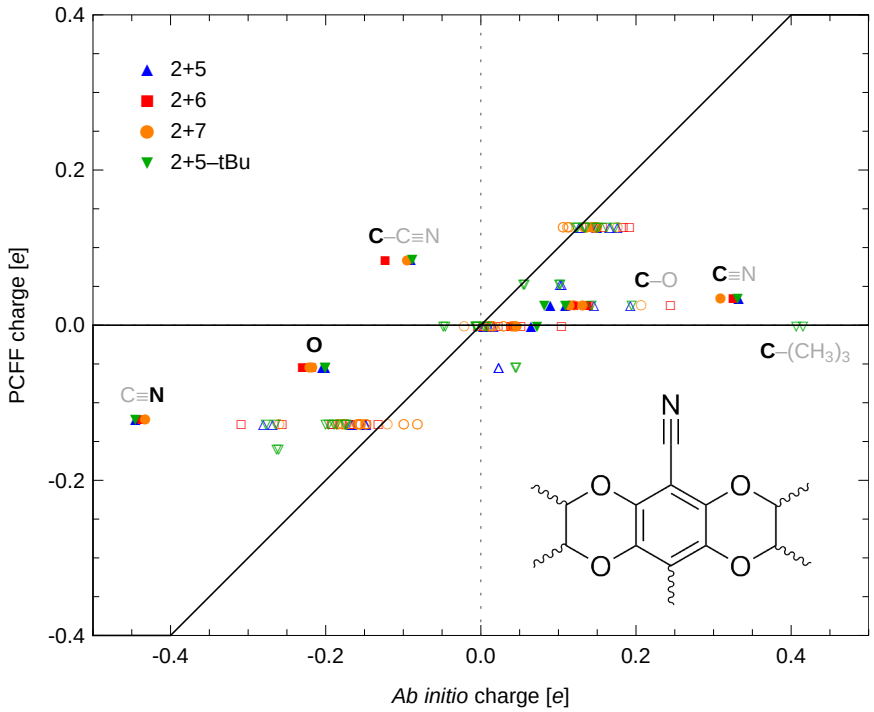

Figure S5. Comparison of charge sets for the biphenyl-core OMIMs series from PCFF and *ab initio* calculations. Charges for the core atoms, which extend out to the oxygen atoms, as shown in the inset chemical structure, are given by closed symbols, while charges for the end-group atoms are given by open symbols.

3.2 Helium pore volumes

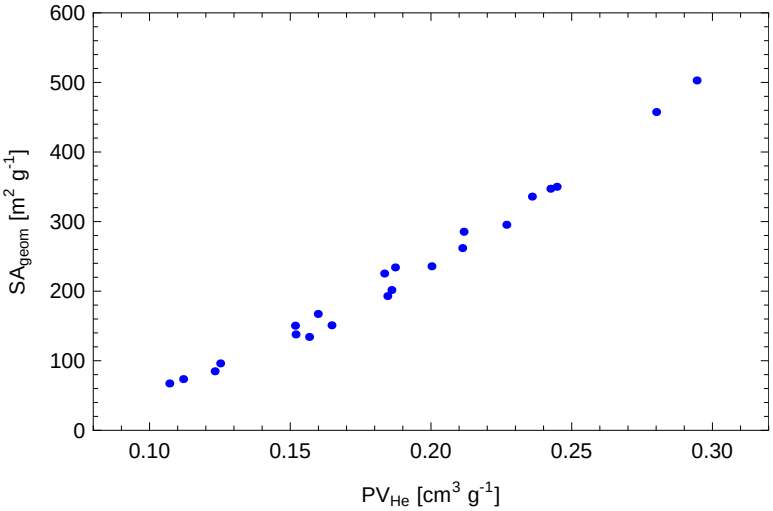

Figure S6. Geometric surface area, SA_{geom}, versus helium pore volume, PV_{He}, for the array of OMIMs.

3.3 Apparent surface areas from BET theory

Table S23 lists the geometric and BET surface areas for the biphenyl-core OMIMs series, which were calculated as described in the methods section. The BET plots yielding the surface areas are also given in Figure S7.

Table S23. Geometric and BET surface areas for biphenyl-core OMIMs

OMIM	SA_{BET} ($\mathrm{m^2\ g^{-1}}$)	SA_{geom} ($\mathrm{m^2\ g^{-1}}$)	$SA_{\mathrm{BET}} - SA_{\mathrm{geom}}$ ($\mathrm{m^2\ g^{-1}}$)
2+5	368	134 (26)	234
2+5–tBu	545	295 (44)	250
2+6	284	85 (26)	199
2+7	383	151 (21)	232

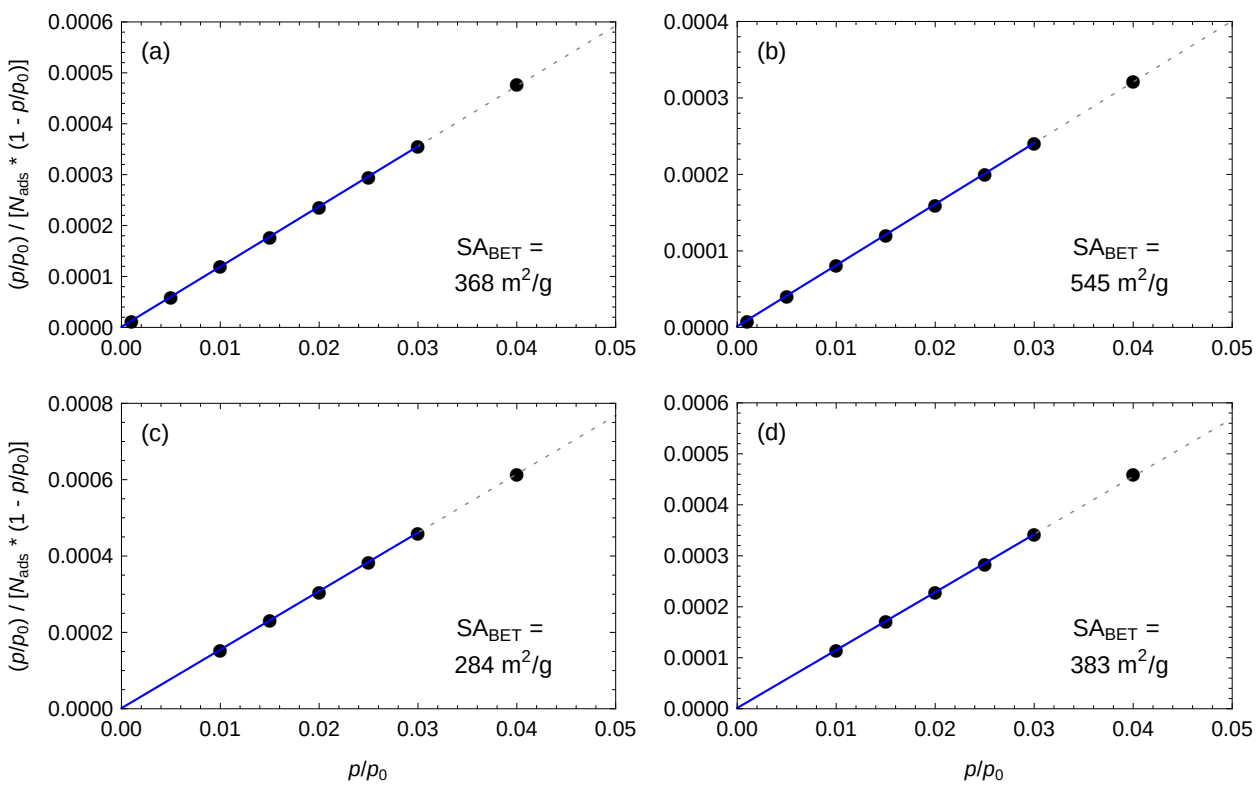

Figure S7. BET plots used to derive apparent surface areas for the biphenyl-core OMIMs: (a) 2+5, (b) 2+5–tBu, (c) 2+6, and (d) 2+7. BET theory was applied over the pressure range $0.01 \leq p/p_0 \leq 0.03$, determined using the consistency criteria.

3.4 Core flexibility measurements

The core flexibility was measured using angles (cores **1** and **4**) and dihedral angles (cores **2** and **3**) from coarse grain beads defined for the core structures, which are illustrated in Figure S8. The beads were defined as the center of mass of the atoms composing the aromatic components, as defined in Table S24 based on the atom numbers given in Figures S1–S4. The angle and dihedral definitions are given in Table S25.

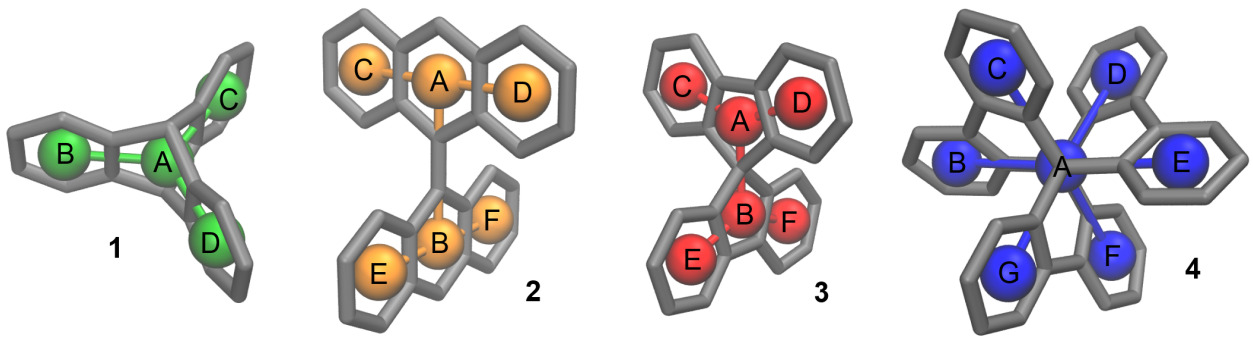

Figure S8. Illustrations of the coarse grain beads defined for the core structures.

Table S24. Definitions of the coarse grain beads for the core flexibility measurements

Bead	**1**	**2**	**3**	**4**
A	1, 2, 7–12	1, 3, 4, 7, 8	1–3, 6, 7	1, 2
B	7, 8, 13, 14, 19, 20	2, 5, 6, 9, 10	1, 4, 5, 8, 9	4, 10, 16, 22, 28, 34
C	9, 10, 15, 16, 21, 22	3, 7, 17–20	2, 6, 10, 14, 18, 22	3, 9, 15, 21, 27, 33
D	11, 12, 17, 18, 23, 24	4, 8, 17–20	3, 7, 11, 15, 19, 23	5, 11, 17, 23, 29, 35
E		5, 9, 17–20	4, 8, 12, 16, 20, 24	6, 12, 18, 24, 30, 36
F		6, 10, 17–20	5, 9, 13, 17, 21, 25	7, 13, 19, 25, 31, 37
G				8, 14, 20, 26, 32, 38

Table S25. Definitions of the core flexibility angles and dihedral angles for each core

Core	Angle definitions					
1	B–A–C	B–A–D	C–A–D			
2	C–A–B–E	C–A–B–F	D–A–B–E	D–A–B–F		
3	C–A–B–E	C–A–B–F	D–A–B–E	D–A–B–F		
4	B–A–D	B–A–F	C–A–E	C–A–G	D–A–F	E–A–G

3.5 Surface areas

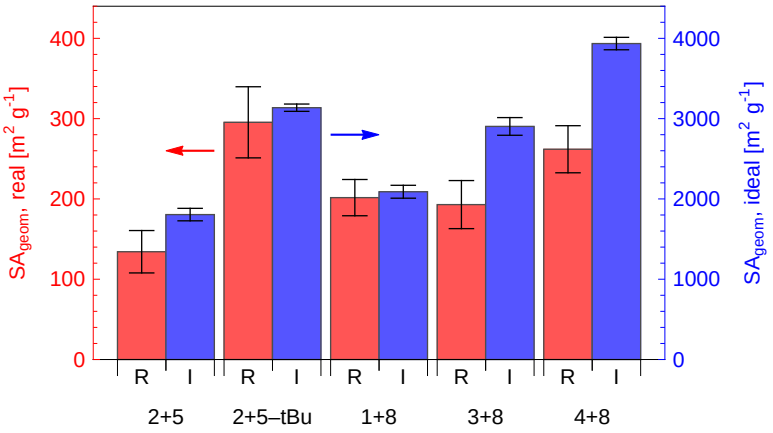

Figure S9. Geometric surface areas, SA_{geom}, for the real (R) and ideal rigid-body (I) simulations of the OMIMs.

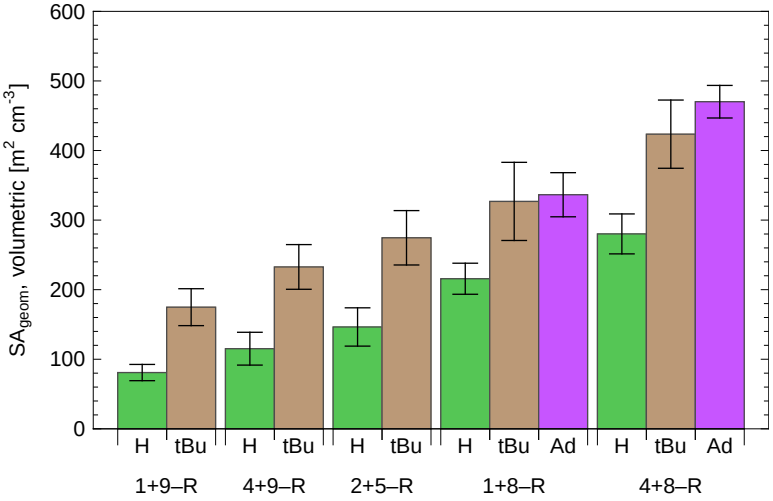

Figure S10. Volumetric geometric surface areas of the *tert*-butyl (tBu) and adamantyl (Ad) functionalized OMIMs.

3.6 Radial distribution functions

The radial distribution functions (RDFs) of the end-group centers are shown for each series of OMIMs in Figure S11. The RDFs of the molecular centers for the propellane- and triptycene-core OMIMs are also given in Figure S12. Lastly, the coordination number can be calculated as the area under the first peak of the RDF, which is shown for example for OMIMs 1+8 and 4+8 in Figure S12d.

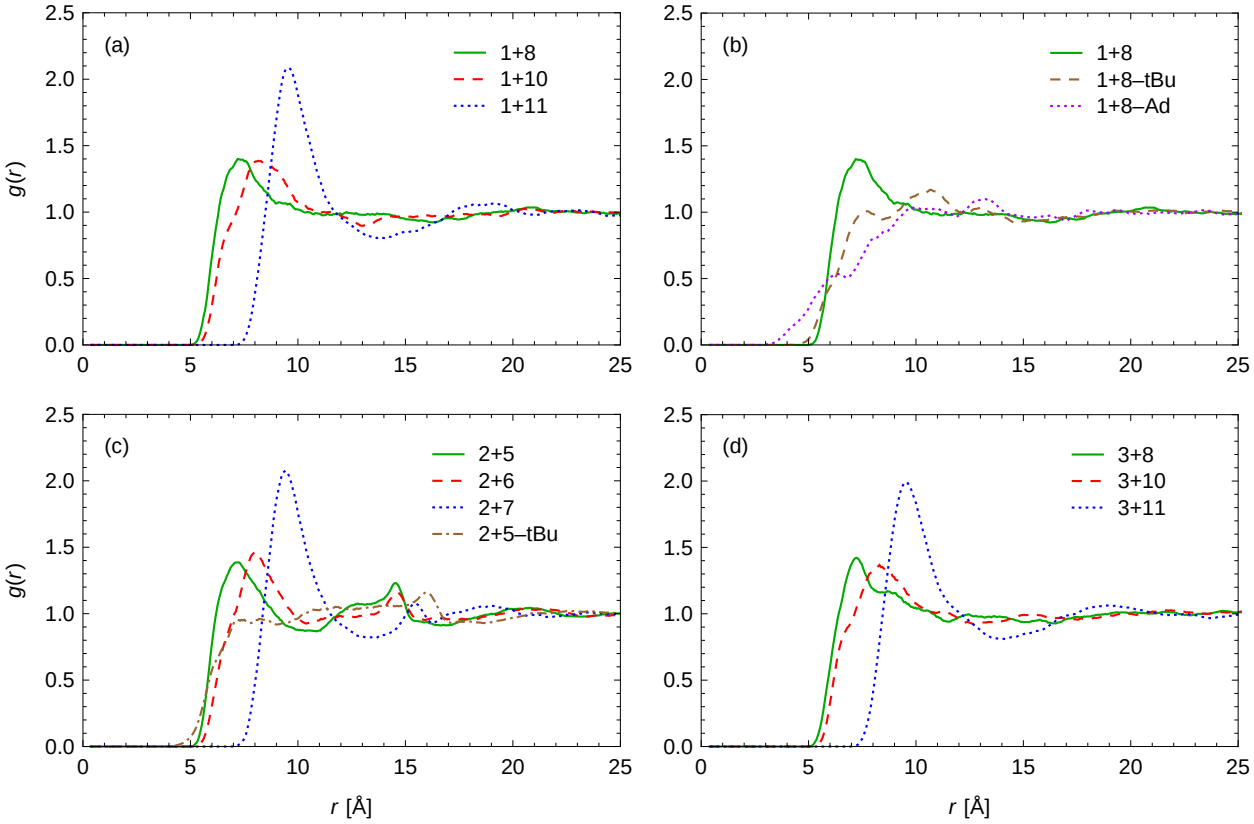

Figure S11. Radial distribution functions of the end-group centers for the (a) triptycene-core OMIMs, (b) OMIM-[1+8–R] series, (c) biphenyl-core OMIMs, and (d) spirobisfluorene-core OMIMs.

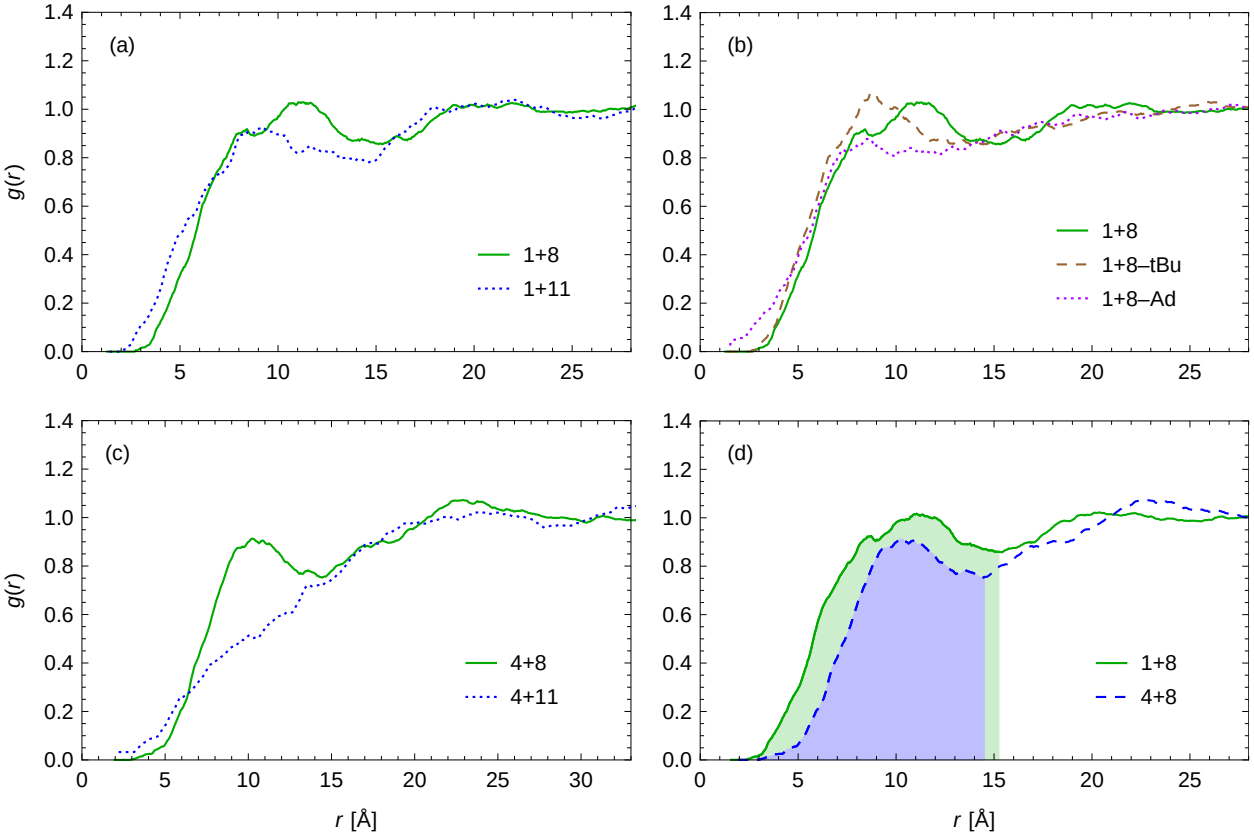

Figure S12. Radial distribution functions of the molecular centers for the (a) triptycene-core OMIMs, (b) OMIM-[1+8–R] series, and (c) propellane-core OMIMs. (d) Derivation of the coordination numbers for OMIMs 1+8 and 4+8 from the area under the first peak of the RDF.

3.7 Structure factors

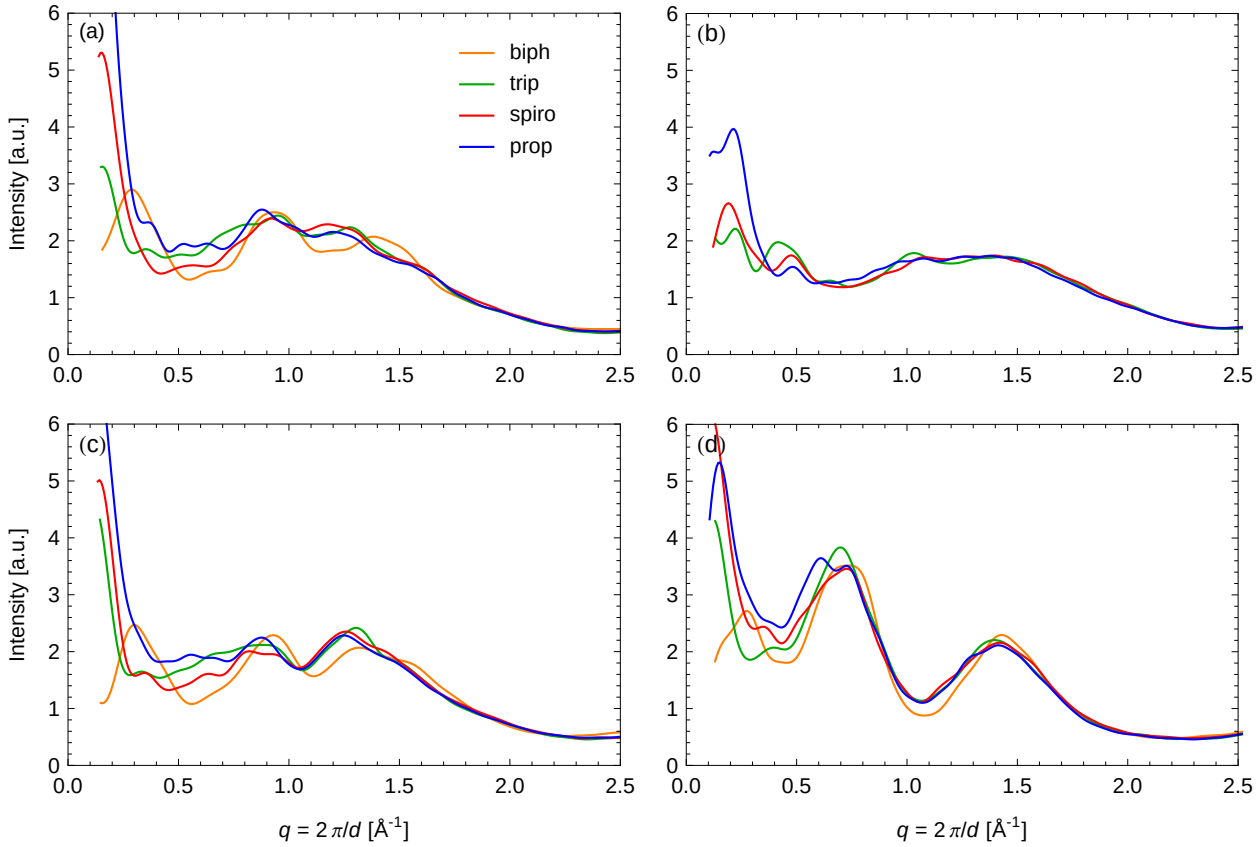

Figure S13. Structure factors for the OMIMs with the (a) triptycene (**5** or **8**), (b) biphenyl (**9**), (c) spirobisfluorene (**6** or **10**) and (d) propellane (**7** or **11**) end groups.

References

[1] Sun, H. *J. Comput. Chem.* **1994**, *15*, 752–768.

[2] Frisch, M. J. et al. Gaussian 03, Revision C.02. 2004.

[3] Bayly, C. I.; Cieplak, P.; Cornell, W.; Kollman, P. A. *J. Phys. Chem.* **1993**, *97*, 10269–10280.

[4] Plimpton, S. *J. Comput. Phys.* **1995**, *117*, 1–19.

[5] Plimpton, S.; Thompson, A.; Crozier, P. Large-Scale Atomic/Molecular Massively Parallel Simulator (LAMMPS). 2012; `http://lammps.sandia.gov`.

[6] Plimpton, S.; Pollock, R.; Stevens, M. Particle-Mesh Ewald and rRESPA for Parallel Molecular Dynamics Simulations. Proceedings of the Eighth SIAM Conference on Parallel Processing for Scientific Computing. New York, 1997.

[7] Abbott, L. J.; Hart, K. E.; Colina, C. M. *Theor. Chem. Acc.* **2013**, *132*, 1334.

[8] Le Roux, S.; Petkov, V. *J. Appl. Crystallogr.* **2010**, *43*, 181–185.

[9] Le Roux, S.; Petkov, V. Interactive Structure Analysis of Amorphous and Crystalline Systems (ISAACS). 2012; `http://isaacs.sourceforge.net`.

[10] Sarkisov, L.; Harrison, A. *Mol. Sim.* **2011**, *37*, 1248–1257.

[11] Martin, M. G. Monte Carlo for Complex Chemical Systems (MCCCS) Towhee, Version 7.0.4. 2010; `http://towhee.sourceforge.net`.

[12] Lüscher, M. *Comput. Phys. Commun.* **1994**, *79*, 100–110.

[13] James, F. *Comput. Phys. Commun.* **1994**, *79*, 111–114.

[14] Potoff, J. J.; Siepmann, J. I. *AIChE J.* **2001**, *47*, 1676–1682.

[15] Brunauer, S.; Emmett, P. H.; Teller, E. *J. Am. Chem. Soc.* **1938**, *60*, 309–319.

[16] Rouquerol, J.; Llewellyn, P.; Rouquerol, F. *Stud. Surf. Sci. Catal.* **2007**, *160*, 49–56.